

# Luminescent Lanthanide-Based Sensor for H<sub>2</sub>O Detection in Aprotic Solvents and D<sub>2</sub>O

Victoria E. Gontcharenko, Alexey M. Lunev, Ilya V. Taydakov, Vladislav M. Korshunov, Andrey A. Drozdov, and Yury A. Belousov 

**Abstract**—Applied methods for detecting water impurities in organic solvents, such as Fischer titration, include wayward equipment and toxic reagents. This method is inapplicable for detecting H<sub>2</sub>O in D<sub>2</sub>O, but suitable techniques like NMR-, IR-, and mass-spectrometry are costly. We report a low-cost, novel luminescent sensor material based on terbium-europium 3D MOF compound developed for facile, portable, and disposable monitoring of water quantities. Our sensor is able to determine water traces in D<sub>2</sub>O and aprotic organic solvents. Treating the material to solvent leads to the change in intensities ratio of terbium and europium bands in emission spectra depending of water content and nature of solvent. For D<sub>2</sub>O calibrating plot  $I_{Eu}/I_{Tb} - \%H_2O$  is linear whereas for dioxane and acetonitrile the dependence becomes linear in the coordinates  $I_{Eu}/I_{Tb} - \ln(\%H_2O)$ . The results reveal the potential application of developed sensor for ratiometric quantitation of H<sub>2</sub>O admixtures in D<sub>2</sub>O, organic solvents, transformer oil, etc.

**Index Terms**—Chemical and biological sensors, optical sensors, luminescent devices.

## I. INTRODUCTION

**D**ETERMINATION of H<sub>2</sub>O concentration in organic solvents, D<sub>2</sub>O and specific media of high practical importance represents a sophisticated problem [1]. The most commonly used Fischer titration method [2] is not able to distinguish H<sub>2</sub>O and D<sub>2</sub>O molecules. Besides, this method uses corrosive and toxic reagents.

Due to the unique luminescent properties of lanthanide complexes, hybrid materials and inorganic compounds are widely used for various applications such as OLED devices

Manuscript received March 2, 2019; revised April 11, 2019; accepted April 29, 2019. Date of publication May 14, 2019; date of current version August 6, 2019. The research was financially supported by the Russian Foundation for Basic Research under Grant 19-03-00263. Spectral measurements were funded by the Russian Scientific Foundation under Grant 17-72-20088. The associate editor coordinating the review of this paper and approving it for publication was Dr. Qiang Wu. (*Corresponding author: Yury A. Belousov.*)

V. E. Gontcharenko, A. M. Lunev, and A. A. Drozdov are with the Chemistry Department, Moscow State University, 119991 Moscow, Russia (e-mail: victo.gontcharenko@gmail.com; lunev94@yandex.ru; drozdov@inorg.chem.msu.ru).

I. V. Taydakov and V. M. Korshunov are with the S. I. Vavilov Department of Luminescence, P. N. Lebedev Institute of Physics RAS, 119991 Moscow, Russia (e-mail: taidakov@mail.ru; vladkorshunov@bk.ru).

Y. A. Belousov is with the Chemistry Department, Moscow State University, 119991 Moscow, Russia, and also with the S. I. Vavilov Department of Luminescence, P. N. Lebedev Institute of Physics RAS, 119991 Moscow, Russia (e-mail: belousov@inorg.chem.msu.ru).

This paper has supplementary downloadable multimedia material available at <http://ieeexplore.ieee.org> provided by the authors. The Supplementary Material contains IR, SEM, EDX, DTA, decay curves, and luminescence spectra. The table of contents is given in the file. This material is 2.61 MB in size.

Digital Object Identifier 10.1109/JSEN.2019.2916498

[3]–[5], bioimaging [6]–[8], banknote anti-counterfeiting protection [9], luminescent thermometers [10]–[12] and sensor materials [13]–[15]. All these tasks are based on common principles but require a specific approach in each case [16]–[18].

A material for liquid sensors should meet a number of requirements: chemical and thermal stability, solvent resistance, well-developed porous structure, intense luminescence, and a “switch on” response [19]. The best way to get a porous sensory material is to create a MOF structure [17], [20], [21]. Azole-containing ligands - derivatives of pyrazole [5], [22], [23], pyrazolone [24]–[26], imidazole [27], [28], triazole [29]–[31] and tetrazole [32], [33] - are known as convenient “building blocks” in the design of effective luminescent lanthanide coordination compounds. It is due to high stability of such heterocycles, additional coordination of rare earth metals (REE) by nitrogen atoms and suitable positions of triplet levels of ligands. 1,2,3-Triazole-4,5-dicarboxylic acid H<sub>3</sub>TDA usually forms highly stable neutral complexes with MOF structure with transition metals [34]. Previously, 3d-4f heterometallic [35]–[39] and pure REE [29], [30], [40] triazolecarboxylates were described. It was shown that a three-dimensional polymer required hydrothermal conditions while a 1D-polymer could be obtained under mild conditions [41], [42]. The deprotonated TDA<sup>3-</sup> ion does not contain luminescence quenchers such as C-H, N-H or O-H bonds.

Europium and terbium ions are the most effective emitters among lanthanides [8], [43]. They demonstrate red and green luminescence, respectively, with the strongest bands at ~615 and ~545 nm. Emission of coordination compounds generally occurs due to energy transfer from an organic ligand, *i.e.*, by the “antenna effect” [43]. The excitation transfer between lanthanides is also possible [44], [45]. In luminescence spectra of heterometallic and mixed-metal complexes, bands related to all constituent REEs can be observed. This property was used in creating white light sources [46] and luminescent thermometers [10]–[12], [47].

The use of the intensity ratio of different bands in luminescence spectra as a sensory response was used earlier [48], including the development of a molecular oxygen sensor [49] and polymer sensors for the determination of water [50] and methanol [51].

In this paper we present a novel, inexpensive, reusable and sensitive material which has been tested as a luminescent sensor for quantitative detection of H<sub>2</sub>O in D<sub>2</sub>O and aprotic

solvents (dioxane and acetonitrile). It represents a mixed-metal 3D MOF based on europium (III), terbium (III) and H<sub>3</sub>TDA, namely [Eu<sub>0.1</sub>Tb<sub>0.9</sub>(TDA)].

## II. EXPERIMENTAL

### A. Apparatus

The CHN composition was estimated with a Vario Macro CHN/CHNS apparatus (Elementar Analysensysteme). XRD patterns were recorded on a D/MAX 2500 diffractometer (Rigaku) in the reflection mode with CuK $\alpha$ 1 ( $\lambda = 1.5406\text{\AA}$ ) radiation and a curved graphite [002] monochromator placed in the reflected beam.

DTA were performed on a Diamond Pyris TG/DTA 2002 tool in air, heating rate 10°/min.

Scanning electron microscopic (SEM) and energy-dispersive X-ray spectroscopic (EDX) studies were carried out on a Leo-Supra 50VP microscope equipped with an Oxford Instruments XMax detector using a 15 kV accelerating voltage and a working distance of 7 nm in a low vacuum mode (N<sub>2</sub>, 40 Pa). A VPSE detector was applied with magnifications from 200 to 2500. EDX spectra were recorded using X-Ray microanalysis and then assigned to the image of sample surface. The energy resolution of the EDX detector reached 129 eV for the MnK $\alpha$  line (5898.8 eV). Statistical analysis of the micrographs for determining the composition of the complexes was performed using ImageJ software.

IR spectra were recorded in the range of 4000–400 cm<sup>-1</sup> in KBr pellets using a PerkinElmer system Spectrum One 100 FTIR spectrometer.

UV-vis spectra were recorded with a LOMO SF-2000 tool in a quartz cell (10.0 mm optical length) relative to water.

High resolution excitation and emission spectra were recorded on a Horiba-Jobin-Yvon Fluorolog 3-22 spectrofluorimeter equipped with a 450 W xenon arc lamp, a flash xenon lamp, double-grating monochromators on both channels and a standard R928 PMT detector. Powdered samples were placed into 2 mm i.d. quartz cells. Life-time experiments were performed on the same setup in a decay-by-delay mode ( $\lambda_{EX} = 300$  nm,  $\lambda_{EM} = 545$  nm for Tb<sup>3+</sup> and 618 nm for Eu<sup>3+</sup>) and subsequently analyzed in the Origin 8.6 Package using an appropriate decay model.

Emission spectra of the material were recorded using an Ocean Optics S2000 spectrometer. A mercury lamp ( $\lambda_{EX} = 312$  nm) was used for luminescence excitation. The duration of signal measurement was 2000 ms and the resulting spectrum was the arithmetic mean of 10 recorded spectra. Then, the spectrum for each sample was treated with baseline subtraction, smoothing with Savitzky-Golay filter and normalization by area of Tb<sup>3+</sup> <sup>5</sup>D<sub>4</sub>-<sup>7</sup>F<sub>5</sub> transition (535-555 nm).

### B. Materials

1,2,3-Triazole-4,5-dicarboxylic acid was synthesized according to a reported procedure [52] by oxidation of 1,2,3-triazole with potassium permanganate KMnO<sub>4</sub> in an aqueous solution (pH = 7) and characterized by IR spectroscopy, CHN and <sup>13</sup>C NMR. A solution of K<sub>3</sub>TDA was prepared by dissolving 15.7 mg (0.1 mmol) H<sub>3</sub>TDA

in 10 ml of 5% KOH and dilution with water to 100 ml. Stock solutions of 0.1 M Ln(NO<sub>3</sub>)<sub>3</sub> (Ln = Eu, Tb) were prepared by dissolving calculated amounts of Ln(NO<sub>3</sub>)<sub>3</sub>·6H<sub>2</sub>O in distilled water. In order to prevent hydrolysis, 1 ml of 1N nitric acid was added to the solutions. Deuterium oxide D<sub>2</sub>O (99.5% Merck) and sodium (Merck) were used as received. Acetonitrile and 1,4-dioxane were degassed and dried according to known literature procedures [53] and stored over 4 $\text{\AA}$  molecular sieves under Ar. Oven-dried (200 °C /12 h) glassware was used for sensing experiments.

### C. Synthesis of Hydrated Complexes

All materials were synthesized by a modified method [29] under same conditions with different proportions of Ln(III) nitrate stock solutions: 1,2,3-triazole-4,5-dicarboxylic acid (78.5 mg, 0.5 mmol) was mixed with sodium hydroxide (40 mg, 1.0 mmol). The mixture was dissolved in 3 ml of water and mixed with 0.1 M of a Ln(III) nitrate stock solution (5 ml, 0.5 mmol). The resulting solution was heated in teflon-lined stainless-steel autoclaves of 10 ml at 165 °C at rate of 50 °C/h, kept at this temperature for 48 hours and cooled at a rate of °C/h.

The {[Ln(TDA)(H<sub>2</sub>O)<sub>3</sub>]\*H<sub>2</sub>O} obtained was separated from the solution by vacuum filtration with Buchner funnel, washed with water, ethanol and diethyl ether and air-dried.

The Eu:Tb ratio was monitored via EDX.

**1** - {[Eu(TDA)(H<sub>2</sub>O)<sub>3</sub>]\*H<sub>2</sub>O}: Yield = 90%; Anal., % Found: C, 13.0; H, 2.5; N, 10.9; C<sub>4</sub>H<sub>8</sub>O<sub>8</sub>N<sub>3</sub>Eu requires: C, 12.7; H, 2.1; N, 11.1. IR: 3700-3000 (broad), 3592, 1604, 1561, 1423, 1377, 1284, 1207, 1152, 1014, 871, 827, 799, 714, 667, 650, 527cm<sup>-1</sup>.

**2** - {[Tb(TDA)(H<sub>2</sub>O)<sub>3</sub>]\*H<sub>2</sub>O}: Yield = 83%; Anal., % Found: C, 12.5; H, 2.4; N, 10.6; C<sub>4</sub>H<sub>8</sub>O<sub>8</sub>N<sub>3</sub>Tbrequires: C, 12.5; H, 2.1; N, 10.9. IR: 3700-3000 (broad), 3650, 3592, 1607, 1560, 1425, 1377, 1287, 1207, 1166, 1153, 874, 837, 800, 715, 668, 530 cm<sup>-1</sup>.

**3** - {[Eu<sub>0.1</sub>Tb<sub>0.9</sub>(TDA)(H<sub>2</sub>O)<sub>3</sub>]\*H<sub>2</sub>O}: Yield = 82%; Anal., % Found: C, 12.5; H, 2.4; N, 10.8; C<sub>4</sub>H<sub>8</sub>O<sub>8</sub>N<sub>3</sub>Eu<sub>0.1</sub>Tb<sub>0.9</sub>requires: C, 12.5; H, 2.1; N, 10.9. Eu:Tb ratio (EDX) 1: 8.97 (Calc. 1: 9.00). IR: 3700-3000 (broad), 3596, 1607, 1559, 1423, 1287, 1207, 1166, 873, 836, 715, 668, 530 cm<sup>-1</sup>.

### D. Dehydration of Complexes

Compounds **1a**, **2a** and **3a** were obtained after vacuum-assisted (0.1 torr) drying of **1**, **2** and **3** respectively at 200 °C for 4h.

**1a**. [Eu(TDA)]: Anal., % Found: C, 15.8; N, 13.7; C<sub>4</sub>O<sub>4</sub>N<sub>3</sub>Eurequires: C, 15.7; N, 13.7 IR: 1591, 1424, 1283, 1150, 1010, 866, 837, 817, 790, 713, 530 cm<sup>-1</sup>.

**2a**. [Tb(TDA)]: Anal., % Found: C, 15.6; N, 13.6; C<sub>4</sub>O<sub>4</sub>N<sub>3</sub>Tbrequires: C, 15.3; N, 13.4. IR: 1585, 1422, 1278, 1149, 1012, 864, 831,818, 789, 713, 530 cm<sup>-1</sup>.

**3a**. [Eu<sub>0.1</sub>Tb<sub>0.9</sub>(TDA)]: Anal., % Found: C, 15.8; N, 13.5; C<sub>4</sub>O<sub>4</sub>N<sub>3</sub>Eu<sub>0.1</sub>Tb<sub>0.9</sub>requires: C, 15.4; N, 13.4. Eu:Tb ratio (EDX) 1: 8.95 (Calc. 1: 9.00) IR: 1587, 1423, 1279, 1149, 1011, 863, 830, 818, 790, 713, 530 cm<sup>-1</sup>.

### E. Sensor Studies

Weighted portions (10 mg) of compound **3a** were transferred to quartz test tubes with 5mm i.d. containing solutions to be analyzed and sealed with silicone septa. Solvent mixtures were obtained by diluting stock solutions until the necessary concentration of H<sub>2</sub>O was achieved. Aliquots, in all cases 200  $\mu$ l, were injected with a syringe through a septum.

## III. RESULTS AND DISCUSSION

### A. Synthesis

Compounds **1-3** were obtained from H<sub>3</sub>TDA, NaOH and REE nitrates under hydrothermal conditions. The use of base allowed to increase the yield from 40-50% in [29] to 82-90%. The effect of synthesis time was also investigated: an increase in time above 48 hours leads to a slight decrease in yield (up to 70%). The identity of the products obtained in [29] is confirmed by a combination of methods of CHN, Powder-XRD, IR-spectroscopy. According to XRD data they have the MOF structure and are isostructural to the known europium 1,2,3-triazole-4,5-dicarboxylate [29] in comparison with powder pattern simulation. Compounds **1a**, **2a**, **3a** were obtained by heating **1-3** *in vacuo*. The compositions of all compounds were confirmed by a set of methods: elemental analysis, IR spectroscopy and DTA. Drying results in a decrease in crystallinity and only weak reflexes can be observed in the XRD patterns of **1a**, **2a** and **3a**(Fig.SI1). Nevertheless, these weak and broadened bands correlate with the data for **1-3**. After treatment with H<sub>2</sub>O, compounds **1a-3a** retain their chemical composition and are identical to the original **1-3** according to IR, CHN and luminescence spectra.

### B. IR Spectroscopy

Determination of water of crystallization in coordination compounds is usually performed by analysis of intensity of stretching and deformation vibrations of OH bonds located in the ranges of 3800-3000 and 1700-1500 cm<sup>-1</sup>. Unfortunately, in both cases the bands in IR spectra are not sufficiently resolved (Figs. S2-S4). Dehydration of **1-3** leads to a decrease in the intensity of the broad band centered at  $\sim$ 3200 cm<sup>-1</sup>. At the same time, weakening of the peak at 3607 cm<sup>-1</sup> which is related to H<sub>2</sub>O molecules engaged in hydrogen bonds is observed. All compounds, including dry **1a-3a**, contain a weak shoulder at 3190 cm<sup>-1</sup>, which might be related to water sorption by the active MOF surface. Deformation vibrations of OH bonds are represented as a weak peak at 1561 cm<sup>-1</sup> that vanishes after dehydrating **1-3** into **1a-3a**. This band overlaps with the bands of deformation vibrations of the C=C bond and  $\nu_{AS}$  of the carboxyl group centered at 1605 cm<sup>-1</sup>. The band at 1424 cm<sup>-1</sup> is related to  $\nu_s$  of COO<sup>-</sup> group and the difference in position with asymmetrical oscillations (181 cm<sup>-1</sup>) proves bridging character of carboxyl coordination. The small shift in the position of the band related to the C=N bond from 798 cm<sup>-1</sup> in **1-3** to 789 cm<sup>-1</sup> in **1a-3a** indicates the involvement of the nitrogen atom in lanthanide coordination after removal of water.

### C. Chemical Composition of Complexes

The chemical structure according to X-ray crystallography as well as the corresponding composition of the europium complex with TDA were reported previously [29]. Unfortunately, the positions of hydrogen atoms and lattice water molecules were not defined in this work. Moreover, the proposed chemical structure [Eu<sub>2</sub>(TDA)<sub>2</sub>(H<sub>2</sub>O)<sub>3</sub>]\*5H<sub>2</sub>O does not match the structure determined from X-ray data ([Eu<sub>2</sub>(TDA)<sub>2</sub>(H<sub>2</sub>O)<sub>6</sub>]). It was revealed that compounds **1-3** were isostructural to the reported europium complex according based on comparison of XPD patterns. Therefore, the exact composition of compounds **1-3** needs to be identified.

The optimal correlation between the experimental elemental analysis data and calculated data for **1-3** corresponds to the composition {Ln(TDA)\*4H<sub>2</sub>O}. Lattice water was also studied by DTA. DTA curves are similar to those presented in paper [29]. According to the DTA data, compounds **1-3** lose water in two stages. In the beginning,  $\sim$ 0.5-1.3 water molecules are lost in the range of 100-180 °C. We assume that not only lattice water, but also a fraction of coordinated water is lost. Then, at 200 °C 2.4 molecules of coordinated water are lost. For the second stage of weight loss, an intense endothermal effect is observed, which confirms the coordination nature of the molecules being lost. The compounds remain stable up to 380 °C and then decompose into a Eu<sub>2</sub>O<sub>3</sub> and Tb<sub>4</sub>O<sub>7</sub>. Thus, we assumed the composition of compounds **1-3** to be {[Ln(TDA)(H<sub>2</sub>O)<sub>3</sub>]\*H<sub>2</sub>O}.

In the range of 100-350 °C, compound **1a-3a** loses about 2-4% of weight which corresponds to the loss of 0.25-0.5 water molecules. This weight loss might be caused by partial hydration of anhydrous **1a-3a** in air. Then, the compounds stay stable and decompose at T > 400 °C. The DTA curves are presented in supplementary information.

Upon UV-radiation, compounds **1**, **2** and **3** intensely emit red, green and orange light respectively. The photoluminescence (PL) spectra of **1-3** are shown in Fig 2. Well-defined sharp lines are related to f-f electron transitions of Eu<sup>+3</sup> and Tb<sup>3+</sup> ions and weak ligand fluorescence can be observed below 500nm. The spectrum of **3** contains emission bands of both Eu<sup>3+</sup> and Tb<sup>3+</sup> ions. The <sup>5</sup>D<sub>0-7</sub>F<sub>0</sub> transition in the spectrum of **1** is not split at room temperature but is slightly broadened which is characteristic of the structure that contains two independent Eu<sup>3+</sup> ions with similar environment [54]. The integral intensity ratio of the hypersensitive transition <sup>5</sup>D<sub>0-7</sub>F<sub>2</sub> and independent magnetic dipole <sup>5</sup>D<sub>0-7</sub>F<sub>0</sub> transition is 2.7, which indicates a relatively high symmetry of the Eu<sup>3+</sup> coordination polyhedron [44]. In the emission spectrum of compound **2**, the integral ratio of the most intense <sup>5</sup>D<sub>4-7</sub>F<sub>5</sub> transition (535-555nm) and the weakest <sup>5</sup>D<sub>4-7</sub>F<sub>3</sub> (605-635) transition is about 0.03 so that the overlap with the Eu<sup>3+</sup> <sup>5</sup>D<sub>0-7</sub>F<sub>2</sub> band is minimal in the spectrum of **3** and allows the usage of the ratio of these bands as an analytical signal. Drying of **1**, **2** leads to compounds **1a**, **2a**, in which the character of the luminescent spectra does not change, but the lines become more broadened. The same correlations apply to compound **3a**, in which, moreover, the Eu/Tb intensity ratio increases due to removal of H<sub>2</sub>O molecules that quench the

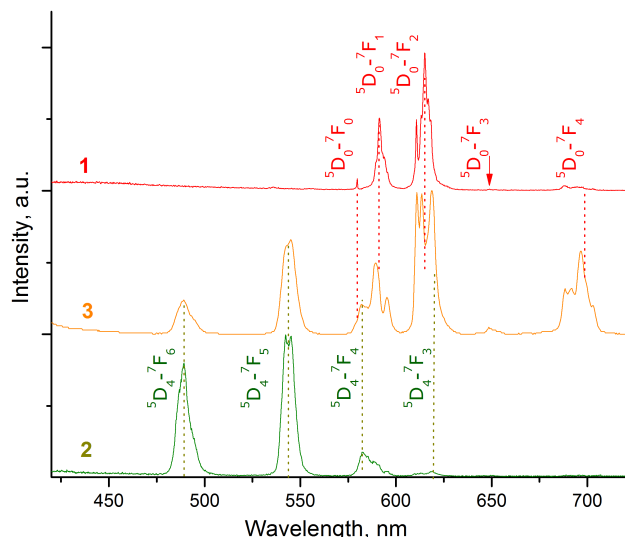


Fig. 1. PL spectra of solid compounds 1-3,  $\lambda_{EX} = 394$  nm for 1, 350 nm for 2 and 3.  $\text{Eu}^{3+}$  and  $\text{Tb}^{3+}$  transitions shown with red and green, respectively.

emission of  $\text{Eu}^{3+}$  in **3**. A summary table containing the positions, intensities and FWHM peaks is given in supplementary information.

#### D. Luminescence and Sensitization

The UV-vis absorption spectrum of  $\text{K}_3\text{TDA}$  (Fig. S13) contains a broad band with a shoulder at 280 nm, and no visible absorption above 300 nm. This behavior is preserved in the excitation spectra of **1-3** (Fig. 2) in the form of a broad band at 270-330 nm and is obviously related to ligand excitation. Besides, these spectra consist of narrow bands of direct excitation of  $\text{Tb}^{3+}$  and  $\text{Eu}^{3+}$  ions. The excitation spectrum of **1** contains peaks related to  $\text{Eu}^{3+}$  only and a wide band corresponding to  $\pi \rightarrow \pi^*$  transitions in the ligand. Moreover, the effectiveness of  $\text{Eu}^{3+}$  excitation through  $^5\text{L}_6 \leftarrow ^7\text{F}_0$  and  $^5\text{D}_2 \leftarrow ^7\text{F}_0$  transitions is higher than through the ligand. Conversely, in the excitation spectrum of **2** direct excitation of  $\text{Tb}^{3+}$  is less effective through  $^5\text{D}_4 \leftarrow ^7\text{F}_6$  and  $^5\text{G}_5 \leftarrow ^7\text{F}_6$  transitions than excitation through the ligand, which indicates decent antenna properties of the  $\text{H}_3\text{TDA}$  ligand for the  $\text{Tb}^{3+}$  ion. The excitation spectra of **3** recorded relative to the luminescence of  $\text{Tb}^{3+}$  and  $\text{Eu}^{3+}$  ions in the mixed-metal coordination compound insignificantly differ in the intensity of the bands that correspond to direct excitation of the  $\text{Eu}^{3+}$  ion. Weak  $^5\text{L}_6 \leftarrow ^7\text{F}_0$ ,  $^5\text{D}_2 \leftarrow ^7\text{F}_0$  and  $^5\text{D}_4 \leftarrow ^7\text{F}_1$  transitions which are observed at  $\lambda_{EM} = 545$  nm in the excitation spectrum of **3** might indicate the existence of a weak energy transfer from  $\text{Eu}^{3+}$  to  $\text{Tb}^{3+}$  either directly or through the ligand. The reverse process of sensitization of  $\text{Eu}^{3+}$  luminescence by  $\text{Tb}^{3+}$  is substantially more effective, as indicated by the bands at  $\lambda_{EX} = 615\text{nm}$  that correspond to  $^5\text{D}_4 \leftarrow ^7\text{F}_6$ ,  $^5\text{G}_5 \leftarrow ^7\text{F}_6$  and other transitions of  $\text{Tb}^{3+}$  in the excitation spectrum of **3**.

Sensitization of  $\text{Eu}^{3+}$  luminescence by  $\text{Tb}^{3+}$  is also confirmed by the decay curves recorded for these ions (Table 1). The determination of lifetimes for the **3** and **3a** is complicated due Tb-to-Eu energy transfer. Only for compounds **1** and **1a**

TABLE I  
T<sub>OBS</sub> OF EUROPIUM AND TERBIUM CENTERED EMISSION, MKS

COMPOUND	EU (618 NM)	TB (545 NM)
1(Eu) or 2(Tb)	292(1)	475(2)
1a(Eu) or 2a (Tb)	388(1)	366(3)
1a(Eu) or 2a (Tb) + H <sub>2</sub> O	296(3)	460(3)
1a(Eu) or 2a (Tb) + D <sub>2</sub> O	712(6)	529(3)
3	n/a	141(1)
3a	n/a	32.2(2)
3a+H <sub>2</sub> O	n/a	60(3); 220(21)
3a+D <sub>2</sub> O	n/a	55.4(7)

that do not contain  $\text{Tb}^{3+}$ ,  $\text{Eu}^{3+}$  decay curves have an exponential character, which allows the determination of lifetimes. **1a** has a slightly higher lifetime than **1** due to removal of OH-quenching during dehydration. Introduction of  $\text{Tb}^{3+}$  to the system (compounds **3** and **3a**) results in a change in the curve character. Moreover, in the initial period at the start of the curve, a rise in the luminescence intensity is observed (Fig.3), which is a direct evidence of the presence of energy transfer in the system [55].

Besides, the  $\tau_{OBS}$  of  $\text{Tb}^{3+}$  in **3** and **3a** is several times lower than in **2** and **2a**. Introduction of  $\text{H}_2\text{O}$  and  $\text{D}_2\text{O}$  molecules differently influences the  $\text{Tb}^{3+}$  and  $\text{Eu}^{3+}$  luminescence, though the emission intensity is higher in both cases. According to the formulae [16],

$$q^{Eu^{3+}} = 1.2 \times \left[ \frac{1}{\tau(\text{H}_2\text{O})} - \frac{1}{\tau(\text{D}_2\text{O})} - 0.25 \right] = 2.07$$

$$q^{Tb^{3+}} = 5 \times \left[ \frac{1}{\tau(\text{H}_2\text{O})} - \frac{1}{\tau(\text{D}_2\text{O})} - 0.06 \right] = 1.12$$

the number of  $\text{H}_2\text{O}$  molecules coordinated to europium and terbium ions less than 3. In the crystal structure reported at [29] hydration number is 3. The difference between these data may be related to particular hydration of 1 and 2 in  $\text{H}_2\text{O}$  and  $\text{D}_2\text{O}$ . The luminescence of  $\text{Eu}^{3+}$  compared with  $\text{Tb}^{3+}$  is quenched by  $\text{H}_2\text{O}$  molecules considerably more strongly [16], [54]. The intricacy of determining the radiative lifetime of the europium ion caused by the excitation transfer interferes with the use of the lifetime as an analytical signal.

#### E. Sensory Signal Measurement and Processing

Several characteristics of luminescence can be chosen as a sensory signal, such as quantum yields, lifetimes and ratio of emission intensities. Measurement of quantum yields is the most complicated among the parameters mentioned above due to difficulties in achieving reproducible results (the determination error is generally higher than 10% [56]). Measuring the luminescence lifetimes is less sophisticated, though in the current work this method can lead to ambiguous results

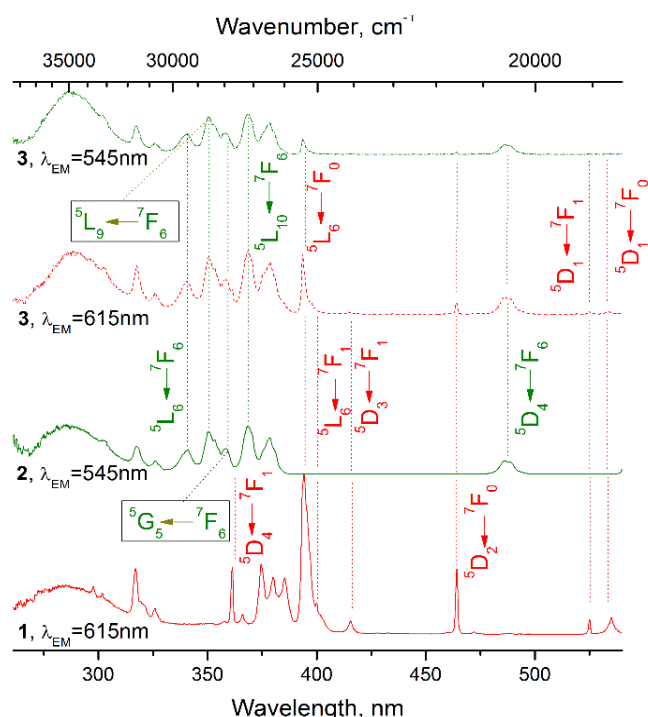


Fig. 2. Excitation spectra of solid 1-3. Eu<sup>3+</sup> and Tb<sup>3+</sup> transitions shown with red and green, respectively.

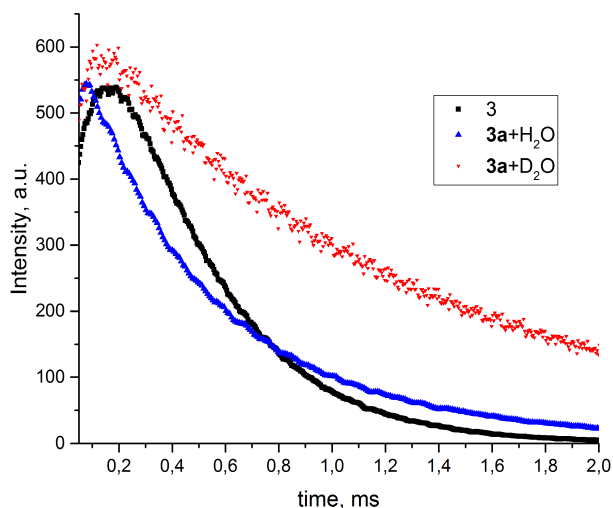


Fig. 3. Decay curves for Eu<sup>3+</sup> emission (618 nm) in solid 3, and suspensions of 3a with H<sub>2</sub>O and D<sub>2</sub>O.

because in compound **3** a non-monoexponential decay curve of Eu<sup>3+</sup> emission is observed, unlike in compound **1**.

#### F. Lifetimes

As a result, the ratio of integral intensities of the main transition of Eu<sup>3+</sup> and Tb<sup>3+</sup> was chosen as an analytic signal in sensory studies. The area of Eu<sup>3+</sup> emission was measured in the range of 605-625 nm (<sup>5</sup>D<sub>0</sub>-<sup>7</sup>F<sub>2</sub> transition) and the area of Tb<sup>3+</sup> emission – in the range of 535-555 nm (<sup>5</sup>D<sub>4</sub>-<sup>7</sup>F<sub>5</sub> transition).

$$S = \frac{I_{Eu}}{I_{Tb}} = \frac{\int_{605}^{625} Id\lambda}{\int_{535}^{555} Id\lambda}$$

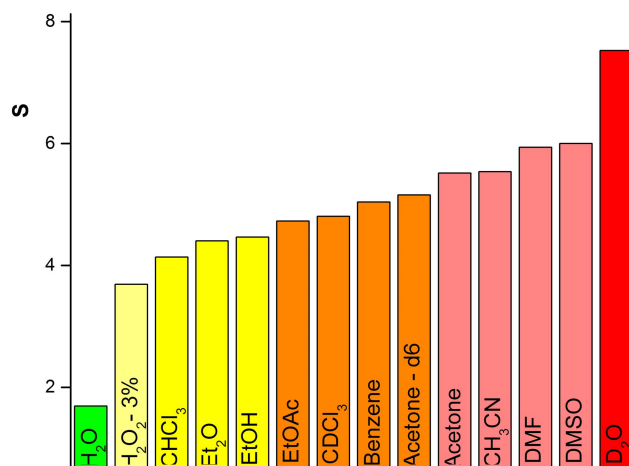


Fig. 4. Dependence of *S* on media for suspension of solid 3a with different solvents.

It is to be noted that at 625 nm, the <sup>5</sup>D<sub>4</sub>-<sup>7</sup>F<sub>3</sub> transition of Tb<sup>3+</sup> takes place. Nevertheless, its integral intensity constitutes about 3% of the main transition (<sup>5</sup>D<sub>4</sub>-<sup>7</sup>F<sub>5</sub>) of the terbium ion. The intensity of emission of <sup>5</sup>D<sub>4</sub>-<sup>7</sup>F<sub>5</sub> transition of Tb<sup>3+</sup> was used as the internal standard as its luminescence is insignificantly affected by -OH quenching [16].

Using different excitation wavelengths (250-390 nm) results in insignificant changes in the ratio of integral intensities of Eu<sup>3+</sup> and Tb<sup>3+</sup> luminescence (Fig.S17). When the compound is exposed to the light source with a wavelength of less than 250 nm, strong ligand fluorescence is observed, while subjecting the material to light of more than 390 nm leads to a cease of Tb<sup>3+</sup> energy sensitization. The highest *S* can be achieved by excitation with 290 and 350 nm, though choosing the latter wavelength leads to a low overall intensity of the compound. Thus, the sensory material was exposed to excitation at 312 nm wavelength, as this available source of light is the closest to 290 nm.

Introducing different solvents to **3a** leads to a change in the ratio of Eu<sup>3+</sup> and Tb<sup>3+</sup> centered emission intensities (Fig. 4 and Fig. S21). The highest decrease in *S* is observed for polar and coordinating solvents, such as water, ethanol, acetone, and acetonitrile. Replacing water with D<sub>2</sub>O leads to a significant increase in *S*, so its value for this media is hardly different from *S* for dry **3a**. For CHCl<sub>3</sub>-CDCl<sub>3</sub> no difference is observed due to the aprotic character of these solvents. For a 3% H<sub>2</sub>O<sub>2</sub> solution a drastic decrease in luminescence intensity is observed. *S* for H<sub>2</sub>O<sub>2</sub> is higher than for H<sub>2</sub>O which may be related to more effective quenching of Tb<sup>3+</sup> emission by peroxide ion or by molecular oxygen.

Studies of the dependence of sensory response on the time after solvent addition show that *S* reaches a plateau after ~2.5 hours (Fig. S8). Such a long time is probably related to the hydration of all ions in a bulky sample rather than to the duration of diffusion. After reaching the plateau, *S* remains constant after 6, 12, 24, and 48 hours.

For the H<sub>2</sub>O-D<sub>2</sub>O mixture, the calibration dependence is linear in the *S*- ω(H<sub>2</sub>O) coordinates in the range of 0.5-100% H<sub>2</sub>O (Fig.5). Studying the sensory signal in

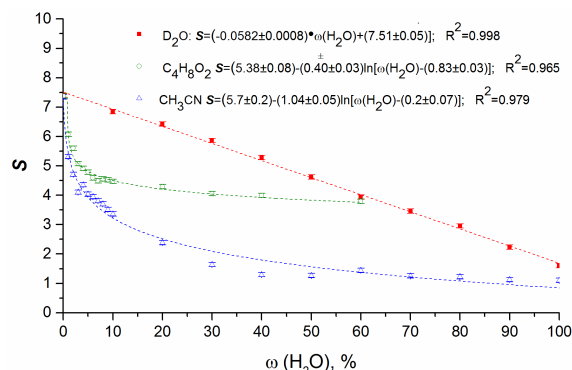


Fig. 5. Calibration charts for the H<sub>2</sub>O-D<sub>2</sub>O (red squares), H<sub>2</sub>O-dioxane (green circles) and H<sub>2</sub>O-CH<sub>3</sub>CN (blue triangles) systems.

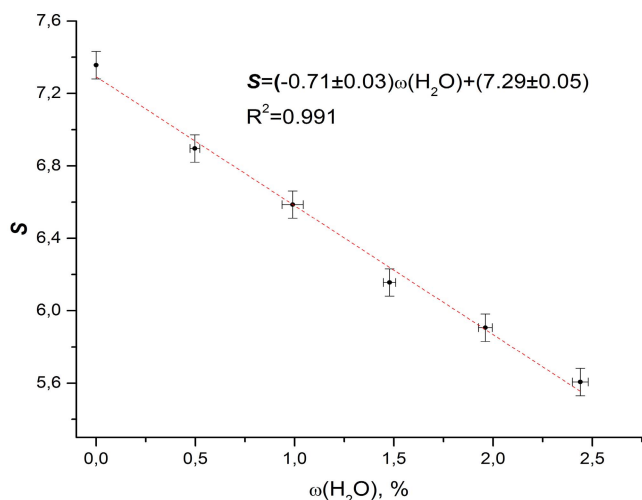


Fig. 6. Calibration chart for determination of H<sub>2</sub>O in D<sub>2</sub>O by the method of standard additions.

solutions with smaller H<sub>2</sub>O concentrations is impossible because higher purity D<sub>2</sub>O (>99.5%) is not available. However, in [50] the calibration dependence is linear from 0 to 12% H<sub>2</sub>O. The high linearity of the calibration curve is caused by the chemical similarity of H<sub>2</sub>O and D<sub>2</sub>O molecules; their small size allows them to enter and exchange in the coordination spheres of all lanthanides. The luminescence color of the sensory material changes gradually from red to yellow with an increase in H<sub>2</sub>O concentration, which makes it possible to distinguish them visually.

For H<sub>2</sub>O-dioxane and H<sub>2</sub>O-CH<sub>3</sub>CN media, the calibration plots become linear in logarithmic coordinates  $S - \ln(\omega(\text{H}_2\text{O}))$  in the range of 0-100% H<sub>2</sub>O in acetonitrile and 0-60% H<sub>2</sub>O in dioxane (Fig. 5).

Moreover, the method of standard additions was used for the determination of H<sub>2</sub>O concentration in the commercially available product – D<sub>2</sub>O (Sigma Aldrich) that was unsealed a long time ago and was used for NMR spectroscopy. Preparation of the sample was conducted in a glove box in order to avoid introducing atmospheric moisture into the sample and distorting the result. The concentration of H<sub>2</sub>O in the added standard solutions was in range of 0.5-2.5 % as the real content of H<sub>2</sub>O was expected to be about 0.5 % (the documented isotopic purity of D<sub>2</sub>O studied was 99.8 % D). The calculated

resulting concentration of H<sub>2</sub>O turned out to be about 2.3% (Fig. 6). An independent analysis by IR spectroscopy gave 2.5%.

#### IV. CONCLUSIONS

In summary, we developed a new sensory material – a mixed-metal 1,2,3-triazole-4,5-dicarboxylate of europium and terbium that can be easily synthesized. The compound obtained is thermally stable up to 380°C, insoluble in water and organic solvents and demonstrates intense simultaneous emission of Eu<sup>3+</sup> and Tb<sup>3+</sup> ions. The compound displays a luminescent sensory response  $S$  caused by the change in the ratio of emission bands of terbium (<sup>5</sup>D<sub>4</sub>-<sup>7</sup>F<sub>5</sub> transition) and europium (<sup>5</sup>D<sub>0</sub>-<sup>7</sup>F<sub>2</sub> transition) ions relative to water molecules. For the H<sub>2</sub>O-D<sub>2</sub>O medium,  $S$  is linear in the range of 0-100% H<sub>2</sub>O ( $R^2 = 0.998$ ), while for the H<sub>2</sub>O-CH<sub>3</sub>CN and H<sub>2</sub>O-dioxane media  $S$  becomes linear in the  $S - \ln(\omega(\text{H}_2\text{O}))$  coordinates ( $R^2 = 0.978$  and  $0.965$ , respectively). This sensory response is caused by selective quenching of europium luminescence by oscillation of OH bonds and a change in efficiency of excitation transfer in the TDA-Tb-Eu system. A determination of H<sub>2</sub>O concentration in commercial D<sub>2</sub>O by the method of standard additions correlates excellently with the result obtained by IR spectroscopy. Thus, the suggested material is promising for the creation of devices for rapid, cheap and reliable quantitative determination of water in organic solvents and D<sub>2</sub>O. Moreover, the suggested material can easily be recovered and reused.

#### APPENDIX

Supplementary data contain IR, SEM, EDX, DTA, decay curves, and luminescence spectra.

#### ACKNOWLEDGMENT

The authors would like to thank Prof. Dr. Yu. S. Pak (D. Mendeleev University of Chemical Technology of Russia) for quantitative determination of H<sub>2</sub>O concentration in D<sub>2</sub>O by IR spectroscopy; to V. E. Kotsyuba and Peoples' Friendship University of Russia for CHN analysis and to Dr. D. I. Petukhov (Moscow State University) for SEM and EDX experiments.

#### REFERENCES

- [1] J. Mitchell and D. M. Smith, *Aquamestry: A Treatise on Methods for the Determination of Water*. (Chemical Analysis), 2nd ed. New York, NY, USA: Wiley, 1984, p. 1366.
- [2] K. Fischer, "Neues Verfahren zur maßanalytischen Bestimmung des Wassergehaltes von Flüssigkeiten und festen Körpern," *Angew. Chem.*, vol. 48, no. 26, pp. 394-396, Jun. 1935.
- [3] F. Zinna, M. Pasini, F. Galeotti, C. Botta, L. Di Bari, and U. Giovannella, "Design of lanthanide-based OLEDs with remarkable circularly polarized electroluminescence," *Adv. Funct. Mater.*, vol. 27, no. 1, Jan. 2017, Art. no. 160371.
- [4] I. V. Taydakov, A. A. Akkuzina, R. I. Avetisov, A. V. Khomyakov, R. R. Saifutayarov, and I. C. Avetissov, "Effective electroluminescent materials for OLED applications based on lanthanide 1.3-diketones bearing pyrazole moiety," *J. Lumin.*, vol. 177, pp. 31-39, Sep. 2016.
- [5] K. M.-C. Wong, M. M.-Y. Chan, and V. W.-W. Yam, "Supramolecular assembly of metal-ligand chromophores for sensing and phosphorescent OLED applications," *Adv. Mater.*, vol. 26, no. 31, pp. 5558-5568, Aug. 2014.

- [6] Y. Yang *et al.*, "Small-molecule lanthanide complexes probe for second near-infrared window bioimaging," *Anal. Chem.*, vol. 90, no. 13, pp. 7946–7952, Jul. 2018.
- [7] M. V. Da Costa, S. Doughan, Y. Han, and U. J. Krull, "Lanthanide upconversion nanoparticles and applications in bioassays and bioimaging: A review," *Anal. Chim. Acta*, vol. 832, pp. 1–33, Jun. 2014.
- [8] S. V. Eliseeva and J.-C. G. Bünzli, "Lanthanide luminescence for functional materials and bio-sciences," *Chem. Soc. Rev.*, vol. 39, no. 1, pp. 189–227, 2010.
- [9] J. F. Suyver and A. Meijerink, "Europium safeguards the euro," *Chemisch2Weekblad*, vol. 98, pp. 12–13, Feb. 2002. [Online]. Available: <https://dspace.library.uu.nl/handle/1874/25831>
- [10] J. Rocha, C. D. S. Brites, and L. D. Carlos, "Lanthanide organic framework luminescent thermometers," *Chem. Eur. J.*, vol. 22, no. 42, pp. 14782–14795, Oct. 2016.
- [11] X. Rao *et al.*, "A highly sensitive mixed lanthanide metal–organic framework self-calibrated luminescent thermometer," *J. Amer. Chem. Soc.*, vol. 135, no. 41, pp. 15559–15564, Sep. 2013.
- [12] C. D. S. Brites *et al.*, "Lanthanide-based luminescent molecular thermometers," *New J. Chem.*, vol. 35, no. 6, pp. 1177–1183, 2011.
- [13] M. Turel, M. Čajlaković, E. Austin, J. P. Dakin, G. Uray, and A. Lobnik, "Direct UV-LED lifetime pH sensor based on a semi-permeable sol-gel membrane immobilized luminescent Eu<sup>3+</sup> chelate complex," *Sens. Actuators B, Chem.*, vol. 131, no. 1, pp. 247–253, Apr. 2008.
- [14] N. A. F. Almeida *et al.*, "Pressure dependent luminescence in titanium dioxide particles modified with europium ions," *Sens. Actuators B, Chem.*, vol. 234, pp. 137–144, Oct. 2016.
- [15] Y. Li, D. Xie, X. Pang, X. Yu, T. Yu, and X. Ge, "Highly selective fluorescent sensing for fluoride based on a covalently bonded europium mesoporous hybrid material," *Sens. Actuators B, Chem.*, vol. 234, pp. 660–667, May 2016.
- [16] D. Parker, "Luminescent lanthanide sensors for pH, pO<sub>2</sub> and selected anions," *Coordination Chem. Rev.*, vol. 205, no. 1, pp. 109–130, Aug. 2010.
- [17] A. B. Aleffi, D. M. Gillen, and T. Gunnlaugsson, "Luminescent/colorimetric probes and (chemo-) sensors for detecting anions based on transition and lanthanide ion receptor/binding complexes," *Coordination Chem. Rev.*, vol. 354, pp. 98–120, Jan. 2018.
- [18] M. L. Aulsebrook, B. Graham, M. R. Grace, and K. L. Tuck, "Lanthanide complexes for luminescence-based sensing of low molecular weight analytes," *Coordination Chem. Rev.*, vol. 375, pp. 191–220, Nov. 2017.
- [19] A. P. de Silva *et al.*, "Signaling recognition events with fluorescent sensors and switches," *Chem. Rev.*, vol. 97, no. 5, pp. 1515–1566, Aug. 1997.
- [20] Y. Cui, B. Chen, and G. Qian, "Lanthanide metal-organic frameworks for luminescent sensing and light-emitting applications," *Coordination Chem. Rev.*, vols. 273–274, pp. 76–86, Aug. 2014.
- [21] C. Pettinari, F. Marchetti, N. Mosca, G. Tosi, and A. Drozdov, "Application of metal–Organic frameworks," *Polym. Int.*, vol. 66, no. 6, pp. 731–744, Jun. 2017.
- [22] M. Metlin, S. Ambrozevich, D. A. Metlina, A. G. Vitukhnovsky, and I. Taydakov, "Luminescence of pyrazolic 1,3-diketone Pr<sup>3+</sup> complex with 1,10-phenanthroline," *J. Lumin.*, vol. 188, pp. 365–370, Aug. 2017.
- [23] A. I. Petrov, M. A. Lutoshkin, and I. V. Taydakov, "Aqueous complexation of Y<sup>III</sup>, La<sup>III</sup>, Nd<sup>III</sup>, Sm<sup>III</sup>, Eu<sup>III</sup>, and Yb<sup>III</sup> with some heterocyclic substituted β-Diketones," *Eur. J. Inorganic Chem.*, vol. 2015, no. 6, pp. 1074–1082, Feb. 2015.
- [24] C. Pettinari *et al.*, "Synthesis of novel lanthanide acylpyrazolonato ligands with long aliphatic chains and immobilization of the Tb complex on the surface of silica pre-modified via hydrophobic interactions," *Dalton Trans.*, vol. 44, no. 33, pp. 14887–14895, 2014.
- [25] Y. A. Belousov and A. A. Drozdov, "Lanthanide acylpyrazolonates: Synthesis, properties and structural features," *Russian Chem. Rev.*, vol. 81, no. 12, pp. 1159–1169, 2012.
- [26] F. Marchetti *et al.*, "Syntheses, structures, and spectroscopy of mono- and polynuclear lanthanide complexes containing 4-acyl-pyrazolones and diphosphineoxide," *Inorganica Chim. Acta*, vol. 363, no. 14, pp. 4038–4047, Nov. 2010.
- [27] Z.-H. Zhang, Y. Song, T.-A. Okamura, Y. Hasegawa, W.-Y. Sun, and N. Ueyama, "Syntheses, structures, near-infrared and visible luminescence, and magnetic properties of lanthanide-organic frameworks with an imidazole-containing flexible ligand," *Inorganic Chem.*, vol. 45, no. 7, pp. 2896–2902, Mar. 2006.
- [28] C. Kachi-Terajima, T. Shimoyama, T. Ishigami, M. Ikeda, and Y. Habata, "A hemiaminal–ether structure stabilized by lanthanide complexes with an imidazole-based schiff base ligand," *Dalton Trans.*, vol. 47, no. 8, pp. 2638–2645, 2018.
- [29] C. J. Chen *et al.*, "3D coordination polymers with chiral structures, [Ln<sub>2</sub>(tda)<sub>2</sub>(H<sub>2</sub>O)<sub>3</sub>·5H<sub>2</sub>O: Hydrothermal synthesis, structural characterization, and luminescent properties," *Zeitschrift für Anorganische Und Allgemeine Chem.*, vol. 638, no. 14, pp. 2324–2328, Nov. 2012.
- [30] G. Yuan, K. Shao, X.-L. Wang, Y.-Q. Lan, D.-Y. Du, and Z.-M. Su, "A series of novel chiral lanthanide coordination polymers with channels constructed from 16Ln-based cage-like building units," *CrystEngComm.*, vol. 12, no. 4, pp. 1147–1152, 2010.
- [31] P. A. Scattergood, A. Sinopoli, and P. I. P. Elliott, "Photophysics and photochemistry of 1,2,3-triazole-based complexes," *Coordination Chem. Rev.*, vol. 350, pp. 136–154, Nov. 2017.
- [32] S. Mal, M. Pietraszkiewicz, and O. Pietraszkiewicz, "Luminescent studies of binuclear ternary europium(III) pyridineoxide tetrazolate complexes containing bis-phosphine oxide as auxiliary co-ligands," *Luminescence*, vol. 33, no. 2, pp. 370–375, Mar. 2018.
- [33] H.-R. Wen, F.-Y. Liang, Z.-G. Zou, S.-J. Liu, J.-S. Liao, and J.-L. Chen, "Mononuclear Dy(III) complex based on bipyridyl-tetrazolate ligand with field-induced single-ion magnet behavior and luminescent properties," *Inorganic Chem. Commun.*, vol. 79, pp. 41–45, May 2017.
- [34] S. Zhang, W. Shi, and P. Cheng, "The coordination chemistry of N-heterocyclic carboxylic acid: A comparison of the coordination polymers constructed by 4,5-imidazoledicarboxylic acid and 1H-1,2,3-triazole-4,5-dicarboxylic acid," *Coordination Chem. Rev.*, vol. 352, pp. 108–150, Dec. 2017.
- [35] J. Y. Zou, W. Shi, N. Xu, H. L. Gao, J. Z. Cui, and P. Cheng, "Cobalt(II)–lanthanide(III) heterometallic metal–organic frameworks with unique (6,6)-connected Nia topologies with 1H-1,2,3-triazole-4,5-dicarboxylic acid: Syntheses, structures and magnetic properties," *Eur. J. Inorganic Chem.*, vol. 2014, no. 2, pp. 407–412, Jan. 2014.
- [36] W. Shi *et al.*, "Synthesis, crystal structures, and magnetic properties of 2D manganese(II) and 1D gadolinium(III) coordination polymers with 1H-1,2,3-triazole-4,5-dicarboxylic acid," *Eur. J. Inorganic Chem.*, vol. 2006, no. 23, pp. 4931–4937, Dec. 2006.
- [37] C. J. Chen *et al.*, "Series of novel 3D microporous heterometallic 3d–4f coordination frameworks with (5,6)-connected topology: Synthesis, crystal structure and magnetic properties," *CrystEngComm.*, vol. 15, no. 23, pp. 4611–4616, 2013.
- [38] X. Jiang, S.-D. Han, R. Zhao, J. Xu, and X.-H. Bu, "Ln<sup>III</sup> ion dependent magnetism in heterometallic Cu–Ln complexes based on an azido group and 1,2,3-triazole-4,5-dicarboxylate as co-ligands," *RSC Adv.*, vol. 5, no. 77, pp. 62319–62324, 2015.
- [39] J. Y. Zou, N. Xu, W. Shi, H.-L. Gao, J.-Z. Cui, and P. Cheng, "A new family of 3d–4f heterometallic coordination polymers assembled with 1H-1,2,3-triazole-4,5-dicarboxylic acid: Syntheses, structures and magnetic properties," *RSC Adv.*, vol. 3, no. 44, pp. 21511–21516, 2013.
- [40] L. Zhang *et al.*, "Three scandium compounds with unsaturated coordinative metal sites—Structures and catalysis," *Eur. J. Inorganic Chem.*, vol. 2015, no. 6, pp. 931–938, Feb. 2015.
- [41] X. Zhang, N. Xu, S.-Y. Zhang, X.-Q. Zhao, and P. Cheng, "From 1D zigzag chains to 3D chiral frameworks: Synthesis and properties of praseodymium(III) and neodymium(III) coordination polymers," *RSC Adv.*, vol. 4, no. 76, pp. 40643–40650, 2014.
- [42] C. Chen, S.-Y. Zhang, H.-B. Song, W. Shi, B. Zhao, and P. Cheng, "One-dimensional lanthanide coordination polymers as promising luminescent materials," *Inorganica Chim. Acta*, vol. 362, pp. 2749–2755, Jun. 2009.
- [43] J.-C. G. Bünzli and C. Piguet, "Lanthanide-containing molecular and supramolecular polymeric functional assemblies," *Chem. Rev.*, vol. 102, no. 6, pp. 1897–1928, May 2002.
- [44] C. Gao *et al.*, "Self-assembly synthesis, structural features, and photophysical properties of dilanthanide complexes derived from a novel amide type ligand: Energy transfer from Tb(III) to Eu(III) in a heterodinuclear derivative," *Inorganic Chem.*, vol. 53, no. 2, pp. 935–942, Jan. 2014.
- [45] A. R. Ramya, D. Sharma, S. Natarajan, and M. L. Reddy, "Highly luminescent and thermally stable lanthanide coordination polymers designed from 4-(Dipyridin-2-yl)aminobenzoate: Efficient energy transfer from Tb<sup>3+</sup> to Eu<sup>3+</sup> in a mixed lanthanide coordination compound," *Inorganic Chem.*, vol. 51, no. 16, pp. 8818–8826, Aug. 2012.

- [46] T. J. Sørensen, M. Tropicano, O. A. Blackburn, J. A. Tilney, A. M. Kenwright, and S. Faulkner, "Preparation and study of an f,f,f' covalently linked tetranuclear hetero-trimetallic complex - a europium, terbium, dysprosium triad," *Chem. Commun.*, vol. 49, no. 8, pp. 783–785, 2013.
- [47] Y. Cui *et al.*, "A luminescent mixed-lanthanide metal-organic framework thermometer," *J. Amer. Chem. Soc.*, vol. 134, no. 9, pp. 3979–3982, Feb. 2012.
- [48] M.-J. Dong, M. Zhao, C. Zou, and C. D. Wu, "A luminescent DyeMOF platform: Emission fingerprint relationships of volatile organic molecules," *Angew. Chem. Int. Ed.*, vol. 53, no. 6, pp. 1575–1579, Feb. 2014.
- [49] T. J. Sørensen, A. M. Kenwright, and S. Faulkner, "Bimetallic lanthanide complexes that display a ratiometric response to oxygen concentrations," *Chem. Sci.*, vol. 6, no. 3, pp. 2054–2059, 2015.
- [50] S. G. Dunning *et al.*, "A sensor for trace H<sub>2</sub>O detection in D<sub>2</sub>O," *Chem.*, vol. 2, no. 4, pp. 579–589, Apr. 2017.
- [51] D.-M. Chen *et al.*, "Ratiometric fluorescence sensing and colorimetric decoding methanol by a bimetallic lanthanide-organic framework," *Sens. Actuators B, Chem.*, vol. 265, pp. 104–109, Jul. 2018.
- [52] G. W. E. Plaut, "The Preparation of 1,5,6-Trimethylbenzotriazole and 1-Methyl-V-triazole-4,5-dicarboxylic Acid," *J. Amer. Chem. Soc.*, vol. 76, no. 22, pp. 5801–5802, Nov. 1954.
- [53] A. J. Gordon and R. A. Ford. *The Chemist's Companion*. New York, NY, USA: Wiley, 1972, p. 429.
- [54] K. Binnemans, "Interpretation of europium(III) spectra," *Coordination Chem. Rev.*, vol. 295, pp. 1–45, Jul. 2015.
- [55] P. A. Tanner and J. Wang, "Energy transfer from Gd<sup>3+</sup> to Tb<sup>3+</sup> in solution," *Chem. Phys. Lett.*, vol. 455, nos. 4–6, pp. 335–338, Apr. 2008.
- [56] H. Ishida, J. C. Bünzli, and A. Beeby, "Guidelines for measurement of luminescence spectra and quantum yields of inorganic and organometallic compounds in solution and solid state (IUPAC Tech. Rep.)," *Pure Appl. Chem.*, vol. 88, no. 6, pp. 701–710, 2016.